Chemico-Biological Interactions 182 (2009) 98–105

Contents lists available at ScienceDirect

Chemico-Biological Interactions

journal homepage: www.elsevier.com/locate/chembioint

Effect of alpha tocopherol acetate in Walker 256/B cells-induced oxidative damage in a rat model of breast cancer skeletal metastases

Riadh Badraoui[a,b], Stéphane Blouin[a], Marie Françoise Moreau[a], Yves Gallois[a], Tarek Rebai[b], Zouhaier Sahnoun[c], Michel Baslé[a], Daniel Chappard[a,*]

[a] INSERM, U 922 – LHEA, Faculté de Médecine, 49045 –>Angers Cedex–>, –>France–>
[b] Laboratoire d'Histologie-Embryologie, Faculté de Médecine, 3029 –>Sfax–>, –>Tunisia–>
[c] Laboratoire de Pharmacologie, Faculté de Médecine, 3029 –>Sfax–>, –>Tunisia–>

ARTICLE INFO

Article history:
Received 6 May 2009
Received in revised form
15 September 2009
Accepted 17 September 2009
Available online 23 September 2009

Keywords:
Bone metastasis
Osteolysis
Osteosclerosis
Metaplasia
Oxidative stress
α-Tocopherol acetate

ABSTRACT

The pathophysiological changes and the oxidative–antioxidative status were evaluated in the bone microenvironment of rat inoculated with Walker 256/B mammary gland carcinoma cells, and used α-tocopherol acetate (ATA) as a countermeasure.

Walker 256/B cells were injected into the right femora of aged male rats. Animals were randomized into three groups: 12 rats were injected with saline (control group); 14 rats were injected with Walker 256/B cells (5×10^4) in the medullar cavity (W256 group); 14 rats were inoculated with Walker 256/B cells and treated with ATA (45 mg/kg BW) (W256 + ATA group). After 20 days, rats were euthanized and the femurs were radiographed. Micro architectural parameters were measured by microcomputed tomography and histology. Serum, bone and bone marrow were evaluated for oxidative damage. In parallel, cell cultures were done in the presence of ATA and ROS were measured by fluorescence; apoptotic cells were determined in parallel. W256 groups had osteolytic damages with marked resorption of cortical and trabecular bone. W256 + ATA animals presented marked osteosclerotic areas associated with tumor necrosis areas inside the bone cavity. Levels of lipid peroxidation and protein oxidation were found to increase in W256 rats; a significant reduction in SOD and GSH-p activities was also observed. W256 + ATA group had significantly reduced oxidative damage, but not reversed back to the control levels. The present study shows that Walker 256/B cells induce skeletal metastases associated with oxidative damage in the bone microenvironment. ATA reduced the oxidative stress damage, enhanced osteosclerosis and tumor cell apoptosis both *in vitro* and *in vivo*.

1. Introduction

Mammary gland carcinoma cells are known to metastasize into a variety of organs including bone. Breast cancer bone metastases are most often characterized as osteolytic and osteosclerotic from a radiological point of view. Osteolytic lesions are due to a marked increase in osteoclast number while foci of osteosclerosis are due to stimulation of osteoblasts by local factors released from the bone matrix [1]. Only 20% of patients with breast cancer are still alive 5 years after the discovery of bone metastasis [2]. The malignant Walker 256/B carcinoma cell line has been proposed as a model for breast cancer skeletal metastases [3–5]. Murine breast carcinoma bears resemblance to human breast cancer because of poor immunogenicity and high metastatic potential [6].

Oxidative stress has emerged as a major pathophysiological mechanism in mediating various disease states and a wide variety of tools are available to monitor this stress [7,8]. At the cellular level, oxidant injury elicits a wide spectrum of responses ranging from proliferation to growth or differentiation arrest, to senescence, and cell death. It has been reported that carcinogenesis stages are influenced by inflammation and oxidative stress [9]. Previous studies have suggested that oxidative stress may provoke cancer initiation and development [10–12].

The antioxidative ability of the vitamin E derivates to suppress tumor growth in preclinical animal models has recently led to

Abbreviations: 2D/3D, two dimensions/three dimensions; ATA, alpha tocopherol acetate; BV/TV, trabecular bone volume; BW, body weight; DCF, 2′,7′-dichlorofluorescein; DMEM, Dulbecco's modified Eagle's Medium; DNPH, 2,4-dintrophenyldrazine; GSH-p, glutathione peroxidase; i.p., intraperitoneal; MDA, malondialdehyde; MicroCT, X-ray microcomputed tomography; PBS, phosphate buffered saline; ROS, reactive oxygen species; SOD, superoxide dismutase; Tb.N, trabecular number; $Tb.P_f$, trabecular bone pattern factor; Tb.Sp, trabecular separation; Tb.Th, trabecular thickness; TBA, 2-thiobarbituric acid; TBARS, thiobarbituric acid reactive substances; TRAcP, tartrate-resistant acid phosphatase; W256, Walker carcinoma 256.

* Corresponding author. Fax: +33 0241 73 58 86.
E-mail address: daniel.chappard@univ-angers.fr (D. Chappard).

0009-2797/$ – see front matter © 2009 Elsevier Ireland Ltd. All rights reserved.
doi:10.1016/j.cbi.2009.09.010

increased interest in their potential use for treating human cancer [6] including other bone diseases such as osteoarthritis [13]. Alpha tocopherol acetate (ATA) is known to possess protective effects against free-radical-induced oxidative tissues damage [14]. The antioxidant role of vitamin E has been implicated in inactivation of harmful free radicals in several pathological states [14,15] including bone diseases associated with increased resorption [16]. Further, oral antioxidant therapy (such as vitamin E, vitamin C, and β-carotene) has been shown to improve efficacy of chemotherapy as adjuvant in bone metastases [17,18].

Possible impairments of the oxidative-antioxidative status induced by breast cancer cells in the bone microenvironment have been poorly explored. The present study was designed to induce osteolytic metastases by intrafemoral inoculation of Walker 256/B cells. The bone microenvironment, oxidative, and antioxidative status were appreciated by lipid and protein oxidation and enzymatic antioxidant level determination. The potent effects of ATA against the oxidative stress were assessed in the metastatic bone microenvironment.

2. Materials and methods

2.1. Chemicals

2-Thiobarbituric acid (TBA), α-tocopherol acetate (ATA), and olive oil were purchased from Sigma–Aldrich Chemical (Illkirsh, France). 2,4-dintrophenyldrazine (DNPH) was purchased from Fluka Co. (Buchs, Switzerland). Dulbecco's modified Eagle's Medium (DMEM), penicillin, streptomycin sulphate, and sodium pyruvate were obtained from Eurobio (Les Ulis, France). Nonessential amino acids and isoflurane were obtained from Cambrex (Walkersville, Md., USA) and AErrane (Baxter S.A., Belgium), respectively; fetal calf serum from Seromed Biochrom (Berlin, Germany). Other chemicals were of analytical grade.

2.2. Cell line and culture conditions

Walker 256/B, a malignant mammary carcinoma cell line capable of inducing bone metastases was used. Cells were kindly provided by Prof. R. Rizzoli (Rehabilitation and Geriatrics, Geneva University Hospitals, Switzerland). These cells were grown in DMEM supplemented with 5% fetal calf serum, 100 UI/ml of penicillin, 100 μg/ml of streptomycin sulphate, 1% of nonessential amino acids, and 1 mM of sodium pyruvate. Cells were cultured at 37 °C in a humidified atmosphere using a water-jacketed 5% CO_2 incubator. To obtain cells with bone trophicity, 10^7 Walker 256/B cells were serially passaged intraperitoneally at 7-day intervals in Sprague–Dawley rats to obtain malignant ascites. After 6 or 7 days, ascitic fluids were collected, and cells in suspension were usable to induce bone metastases.

2.3. Animals

Forty male Sprague–Dawley rats (Harlan, Gannat, France) were bred under well-controlled conditions (24 °C and a 12-h/12-h light/dark cycle). Their age was 8–10 weeks on the day of surgery.

Rats were randomly divided into three groups: (i) control group: 12 rats received an intrafemoral injection of saline; (ii) W256 group: 14 rats received an intrafemoral inoculation of Walker 256/B cells (5×10^4); and (iii) W256 + ATA group: 14 rats having received an intrafemoral inoculation of Walker 256/B as above and were treated 6 days/week with ATA. ATA (dissolved in olive oil) was administered by gavage at a final concentration of 45 mg/kg BW and the treatment began on the day after surgery. Rats were given free access to conventional laboratory diet (UAR, Villemoison sur Orge, France) and water ad libitum all along the study. The Animal Care and Use committee of the University of Angers (France) approved all procedures.

2.4. Surgical procedure

All animals were anesthetized with ketamine (100 mg/kg i.p.) and xylazine (10 mg/kg i.p.). Bilateral superficial incisions were made in the skin after disinfection with 70% ethanol. Additional incisions were cut along the patellar ligament to expose the femoral diaphysis with minimal damage. Walker 256/B cells (10^4 in 10 μl of culture medium) were slowly injected into the medullar cavity of the right femur. To prevent the malignant cells from leaking out, the injection site was closed with bone wax. Rats of the control group were anesthetized and received 10 μl of saline without malignant cells in the medullar cavity. The wound was then closed by using metal skin clips. Twenty days after surgery, animals were euthanized (this duration has been determined by preliminary studies to be sufficient to obtain bone metastases) [3]. Femurs were dissected and the adhering muscles were removed.

In each group, half of the animals were used to measure the oxidative/antioxidative status by biochemical analyses; the remaining half was used for radiographic and histological evaluation. In each animal, biochemical analyses were done, (i) on the femoral bone marrow (bone marrow) obtained after flushing; (ii) on bone, after mincing and homogenization (100 mg/ml) at 4 °C in 0.1 mol/l Tris–HCl buffer pH 7.4 and centrifugation at 3000 rpm for 10 min. The supernatant was collected for biochemical assays; (iii) on blood, taken from heart puncture and centrifuged for 20 min at 4000 rpm. Separated serums were kept frozen at −80 °C.

Radiological and histological analyses were done on femurs fixed in a formalin–alcohol based fluid at +4 °C during 24 h.

2.5. Bone radiographs

Radiographs were performed using a Faxitron X-ray system (Edimex, Angers, France) with a 5 cm × 5 cm CCD camera which provides digitized Images 1024 × 1024 pixels large in the TIF format (Tagged-Image File format). The accelerating voltage was fixed at 30 kV, 30 mA with a 9-s exposure time; the gain and offset were maintained at the same levels for the whole series of bones. The distance between the X-ray tube and the camera was constant and mechanically provided by the apparatus shelf with a magnification of 5×.

2.6. X-ray microcomputed tomography

The distal femurs were scanned with a Skyscan 1072 X-computed microtomograph (Skyscan, Kontich, Belgium) using a microfocus X-ray tube (80 kV/100 μA). Bone samples were analyzed at a magnification of 36× (one pixel corresponding to 8.61 μm) with the cone beam procedure using a 1-mm aluminum filter. For each sample, a stack of 350 section images was 3D reconstructed covering 2.9 mm. The 3D models were reconstructed from the stack with a surface-rendering program (Ant, release 2.2, Skyscan) after interactive segmentation. The volume of interest was designed by drawing polygons on the 2D gray sections.

Trabecular bone volume (BV/TV, in %), trabecular number (Tb.N, in mm^{-1}), trabecular separation (Tb.Sp, in μm), trabecular thickness (Tb.Th, in μm), and trabecular bone pattern factor ($Tb.P_f$) were calculated from 3D models of the metaphyseal region. An interesting tool of the ANT software allows re-slicing of the 3D models across a plane positioned in a specified direction (vertical and parallel to the long axis of the bone). $Tb.P_f$ is mainly based on the use of mathematical morphology in image analyzer systems [19]. The rational of the method is supported by the observation that, the $Tb.P_f$ performed provides low values in a well-connected net-

work and high values when marked disconnection of trabeculae is present [20].

2.7. Histopathology

Histological analysis was performed on bone sample of three groups. They were embedded undecalcified in methylmethacrylate. Sections were cut dry (7 μm thick) parallel to the axis of the bone core on a heavy-duty dry microtome equipped with 50° tungsten carbide knifes (Leica Polycut S, Rueil-Malmaison, France). Sections were stained with a modified Goldner's trichrome [21].

2.8. Biochemical study of the oxidative stress

2.8.1. Thiobarbituric acid reactive substances (TBARS) level

Lipid peroxidation in bone and bone marrow was assessed by the method of Devasagayam and Tarachand [22]. The incubation medium consisted of 1 ml of 0.15 mol/l Tris–HCl buffer (pH 7.4), 0.3 ml of 10 mmol/l KH_2PO_4 and 0.2 ml of tissue extraction in a total of 2 ml. Tubes were incubated at 37 °C with constant shaking. After 20 min the reaction was stopped by the addition of 1 ml of 10% trichloroacetic acid. The tubes were then shaken, 1.5 ml of TBA added and tubes were heated for 20 min in a boiling water-bath. TBA reacts with malondialdehyde (MDA) and MDA-like substances producing a pink pigment with an absorption maximum at 532 nm.

Serum TBARS levels were determined with a spectrophotometric method [23]. 100 μL of serum was mixed with 1 mL 0.67% TBA and 500 μL of 20% TCA. The mixture was incubated at 100 °C for 20 min. After cooling, it was centrifuged at 12,000 × *g* for 5 min and the absorbance was measured.

2.8.2. Protein oxidation

Proteins carbonyls in the bone and bone marrow were determined using a spectrometric DNPH assay according to Fagan et al., with minor modifications [24]. Tissues were homogenized using a cell lysis buffer containing PBS (pH 7.2), 1% Triton X-100, 1 mM EDTA and 1× protease inhibitor cocktail; insoluble cell debris were removed by centrifugation. Aliquots of protein samples were precipitated with 10 volumes of HCl-acetone (3:100) and then washed with 5 ml of 10% of TCA solution. Pellets were resuspended in 500 μl buffer solution and then reacted with 500 μl of 10 mM DNPH (in 2 M HCl) by vortexing for 15 min. To remove the unreacted DNPH, the centrifuged pellets were washed with 5 ml of 20% TCA and 5 ml of ethanol:ethylacetate mixture (v/v; 1:1). The final precipitate was resolved in 1 ml of 6 M guanidine HCl, and absorbance at 380 nm was determined for the sample treated with DNPH and HCl. The carbonyl content was calculated from the absorbance measurement at 380 nm and absorption coefficient $\varepsilon = 22{,}000\ M^{-1}\ cm^{-1}$.

2.8.3. Catalase antioxidant assay

Catalase activity was determined by the kinetic assay following the method of Beers and Sizer in which the disappearance of peroxide is monitored spectrophotometrically at 240 nm [25]. One unit of catalase is equivalent to the amount of protein necessary to decompose 1 μmol of H_2O_2 per minute. The extinction coefficient of H_2O_2 used was $43.6\ M^{-1}\ cm^{-1}$.

2.8.4. Glutathione peroxidase (GSH-p) antioxidant assay

Tissues samples were homogenized with ice-cold 150 mM KCl. Glutathione peroxidase was determined by a spectrophotometric method based on the use of Ellman's reagent [26]. This method assay records the disappearance of NADPH at 340 nm.

2.8.5. Superoxide dismutase (SOD) antioxidant assay

SOD activity was determined by the method of McCord and Fridovich [27]. This method assay depends on the SOD activity to inhibit cytochrome C reduction mediated by the $O_2^{\bullet -}$ generated. SOD activity was monitored spectrophotometrically at 505 nm.

2.9. Cell culture

For biochemical experiments, cells were cultured as above described. Cell viability was assessed by trypan blue dye prior to all treatments. Cells were seeded in 24-well cell culture plates at a concentration of 5×10^4 cells/ml/well. Each well contained a sterilized microscope coverglass where cells were allowed to adhere for about 24 h before the medium exchange and treatment with α-tocopherol acetate.

2.9.1. Treatment procedure with ATA

20 μl aliquots of ATA dissolved in absolute ethanol were added to the wells to give final concentrations of 2.5 or 5 μg/ml. The control wells received 20 μl of ethanol solution. Application of these doses was largely based on early study in prostate cancer cells [28]. Walker 256/B cells were incubated with ATA at 37 °C at different concentrations or for different incubation periods: 24, 48, or 72 h. These samples were processed for analysis of ROS generation, by measurement of DCF fluorescence intensity, and Hoechst staining assay to assess apoptosis on the basis of DNA fragmentation.

2.9.2. ROS measurements by DCF assay

The fluorescent method detection of ROS, specifically hydrogen peroxide (H_2O_2) was carried out using fluorescent probe 2′,7′-dichloro-dihydrofluorescein diacetate. The hydrolyzed product is a nonfluorescent analog, 2′,7′-dichlorofluorescene which is trapped in the cell. In the presence of certain oxygen free-radical intermediates, such as H_2O_2 or low-molecular weight peroxyl radicals, it is oxidized to the highly fluorescent 2′,7′-dichlorofluorescein (DCF) [29,30].

Briefly, cells were harvested, washed twice with PBS and resuspended in serum free medium. Loaded with 100 μM of 2′,7′-dichloro-dihydrofluorescein diacetate; cells were incubated at room temperature in the dark for 30 min. The intensity of DCF was measured using a TECAN spectrofluorometer ($\lambda_{exc} = 485$ nm, $\lambda_{em} = 535$ nm). Each experiment was performed in triplicate. As a positive control, cells were separately treated with H_2O_2 and processed for ROS detection.

2.9.3. Apoptosis measurement by Hoechst 33342 staining assay

Apoptosis was assessed by Hoechst 33342 staining (Apoptosis-Hoechst staining kit; Beyotime Biotechnology, China) on the basis of DNA fragmentation. Briefly, cells were immersed in 0.5 ml of methanol for 15 min, followed by two rinses with PBS. Then cells were stained with Hoechst 33342 (1 μg/ml of distilled water) in a dark chamber for 10 min and rinsed twice in PBS again. Cells were analyzed by fluorescence microscopy using excitation 348 nm/emission 480 nm wavelengths; the apoptotic cells and fragmented pycnotic nuclei emitting intense fluorescence. Four hundred well-spread cells were randomly analyzed for apoptosis from each sample. Apoptotic cells, with nuclear DNA fragmentation, were recorded and expressed as percentage.

2.10. Statistical analysis

Statistical analysis was performed using the Prism software package (GraphPad, San Diego, CA). Data are expressed as the mean and the standard error of the mean (SEM). An analysis of variance was used to compare the differences between the groups. Newman–Keuls post hoc test was performed. Statistical significance was defined as $p < 0.05$.

Table 1
Histomorphometric parameters obtained by microCT.

	Sham	W256	W256 + ATA
BV/TV (%)	11.26 ± 1.6	2.33 ± 0.47[a,c]	8.67 ± 1.45[b]
Tb.P_f	3.6 ± 1.6	14.2 ± 1.0[a,c]	6.2 ± 1.4[b]
Tb.Th (μm)	136 ± 8	119 ± 4[a]	150 ± 7[b]
Tb.N (/mm)	0.80 ± 0.08	0.19 ± 0.03[a,c]	0.56 ± 0.08[a,b]
Tb.Sp (μm)	1272 ± 55	1725 ± 70[a,c]	1440 ± 95[a,b]

[a] Statistical significance of the difference: $p < 0.05$ versus sham group.
[b] Statistical significance of the difference: $p < 0.05$ versus W256 group.
[c] Statistical significance of the difference: $p < 0.05$ versus W256 + ATA group.

3. Results

All animals injected with Walker 256/B cells were found severely ill. Clinical impression of the animals' health and well-being was obtained daily in the 3 groups when checking the animals for clinical signs (rough hair coat, hunched back, and apathy). Palpation of the injected leg was done twice per week to check for the presence of thigh enlargement. On X-ray examinations, rats of the W256 group developed an osteolytic metastasis at the injected site. Cortical lytic bone lesions were evidenced on X-ray with an extension to the soft tissues. This represents a sign of gravity since cortical perforations may lead to pathological fractures.

Woven bone was often observable in the subperiosteal area with an extension into the vicinal muscles. Areas of bone resorption were evidenced in the whole bone metaphysis and predominated under the growth plate.

Similarly, rats of the W256-ATA group developed osteolytic areas but the extent of resorption foci was more limited. In several animals, mixed lesions were observable with foci of sclerosis appearing as low calcified spots on the X-rays.

Histomorphometric analysis by microCT evidenced a massive bone loss in the W256 group with a reduced bone volume associated with a marked reduction in the number of trabeculae (Table 1). The metastasis considerably affected trabecular microarchitecture with an increase in Tb.Sp, a thinning of trabeculae due to resorption and a loss of connectivity (Fig. 1A). When 3D models were re-sliced, 2D sections performed along the femoral axis evidenced a marked disorganization of the primary and secondary spongiosa, the frequent erosion of the growth plate and disorganization of the trabecular network of the epiphysis. Cortical perforations were also found, particularly at the perichondral groove of Ranvier (a thin collar of bone that limits the lateral side of the growth plate). Some metaplastic bone was often observed in the periosteal envelope.

In the W256 + ATA group, the bone volume was not significantly reduced when compared to the control group but was significantly higher than in W256 animals. Microarchitecture was significantly different from both control and W256 rats: trabecular number was decreased and Tb.Sp increased. Taken together, this would tend to imply that ATA had a partial protective effect on bone mass and microarchitecture. However, the trabeculae were difficult to threshold on the 2D sections in this group and packets of poorly calcified bone seemed slightly detached from the background noise. When re-slicing was done, sections parallel to the long axis of the femur evidenced numerous foci of metaplastic bone with a very low calcium charge. These foci cannot be properly segmented from images either for histomorphometry or 3D reconstruction.

On histological sections, tumor cells had invaded the whole femoral shaft of the W256 rats and almost completely resorbed the growth plate. Tumor cells were also evidenced in the epiphysis (Fig. 1B). In these areas, an increase in the amount of TRAcP osteoclasts was observed. Metaplastic bone was observed in the periosteal envelope. In the W256-ATA group, treatment prevented, even in part, the resorption and disorganization of the growth cartilage (Fig. 1B and C). The amount of metaplastic bone differed considerably from rat to rat. Some rats had a dramatic increase in the amount of woven bone, in the center of the secondary spongiosa; others had limited foci in the vicinity of the tumor cells. In most cases, the woven bone appeared in the form of very thin trabeculae, some of them only composed of osteoid tissue. The tumor mass was reduced in almost all animals in the center of the bone with foci of tumor cell necrosis; on the contrary, tumor cells appeared more developed outside the femoral shaft with an extension in the muscle and soft tissues.

Biochemical analysis found that TBARS levels and carbonyl contents were significantly increased in bone marrow, serum and bone (Fig. 2A and B, respectively) of rats with skeletal metastases of the W256 and W256-ATA groups. Levels of antioxidant in bone, bone marrow, and serum are depicted in Table 2. The W256 group showed significantly depletion of SOD activity in bone and bone marrow. GSH-p levels were also significantly decreased in bone and bone marrow of rats of the W256 group. In spite of the significantly increased peroxidated compounds observed in the serum (TBARS and carbonyl content), there was no significant change in the activity of GSH-p between the W256 group and the control group. Catalase levels did not show statistical differences between the three groups.

Treatment with ATA modulated lipids and protein oxidation significantly only in the bone marrow since TBARS and carbonyl content levels were significantly decreased (respectively $p < 0.05$ and 0.01 versus the W256 group) (Fig. 2A). Carbonyl content levels were reversed back to the control levels in bone and serum (Fig. 2B). Table 2 shows that ATA seemed to normalize the levels of SOD and GSH-p.

ROS in cell cultures were evaluated using the fluorescent technique and 2′,7′-dichloro-dihydrofluorescein diacetate as fluorescent probe. A considerable decrease of ROS releasing was evidenced on Walker 256/B cells treated with ATA (at doses of 2.5 or 5 μg/ml) compared to control, regardless of the duration of treatment (Fig. 3A). Cell apoptosis was assessed on the basis of DNA fragmentation. No statistical difference was noted after 24 h of treatment. ATA induced a dose dependant increase in the number of apoptotic cells after 48 h and the effect was more pronounced at 72 h (Fig. 3B).

4. Discussion

Bone is the main site of metastases for breast and prostate cancers; it provides an especially fertile "soil" to this kind of cells according to the "seed and soil" theory [31]. Local inoculation of

Table 2
Specific activities of superoxide dismutase (SOD), catalase, and glutathione peroxidase (GSH-p) in SD rats following inoculation of 10^4 Walker 256 cells with or without ATA treatment.

	Controls, $n = 6$	W256, $n = 7$	W256 + ATA, $n = 7$
SOD (U/mg)			
Serum	26.4 ± 1.2	33.3 ± 1.8[a]	29.7 ± 1.4
Bone	17.9 ± 1.7	10.2 ± 0.9[a]	14.1 ± 2.1
Bone marrow	10.3 ± 0.9	5.9 ± 0.7[a]	8.1 ± 0.0
Catalase (U/g)			
Serum	2.3 ± 0.2	1.5 ± 0.2	1.7 ± 0.3
Bone	7.9 ± 1.4	8.9 ± 1.6	8.9 ± 1.5
Bone marrow	4.1 ± 0.3	4.1 ± 0.4	4.2 ± 0.5
GSH-p (U/mg)			
Serum	27.3 ± 1.1	33.3 ± 1.8	30.8 ± 2.1
Bone	17.9 ± 1.1	10.8 ± 0.9[a,c]	15.2 ± 0.7[b]
Bone marrow	27.5 ± 1.3	21.9 ± 0.7[a]	24.9 ± 1.7

[a] Statistical significance of the difference: $p < 0.05$ versus Sham group.
[b] Statistical significance of the difference: $p < 0.05$ versus W256 group.
[c] Statistical significance of the difference: $p < 0.05$ versus W256 + ATA group.

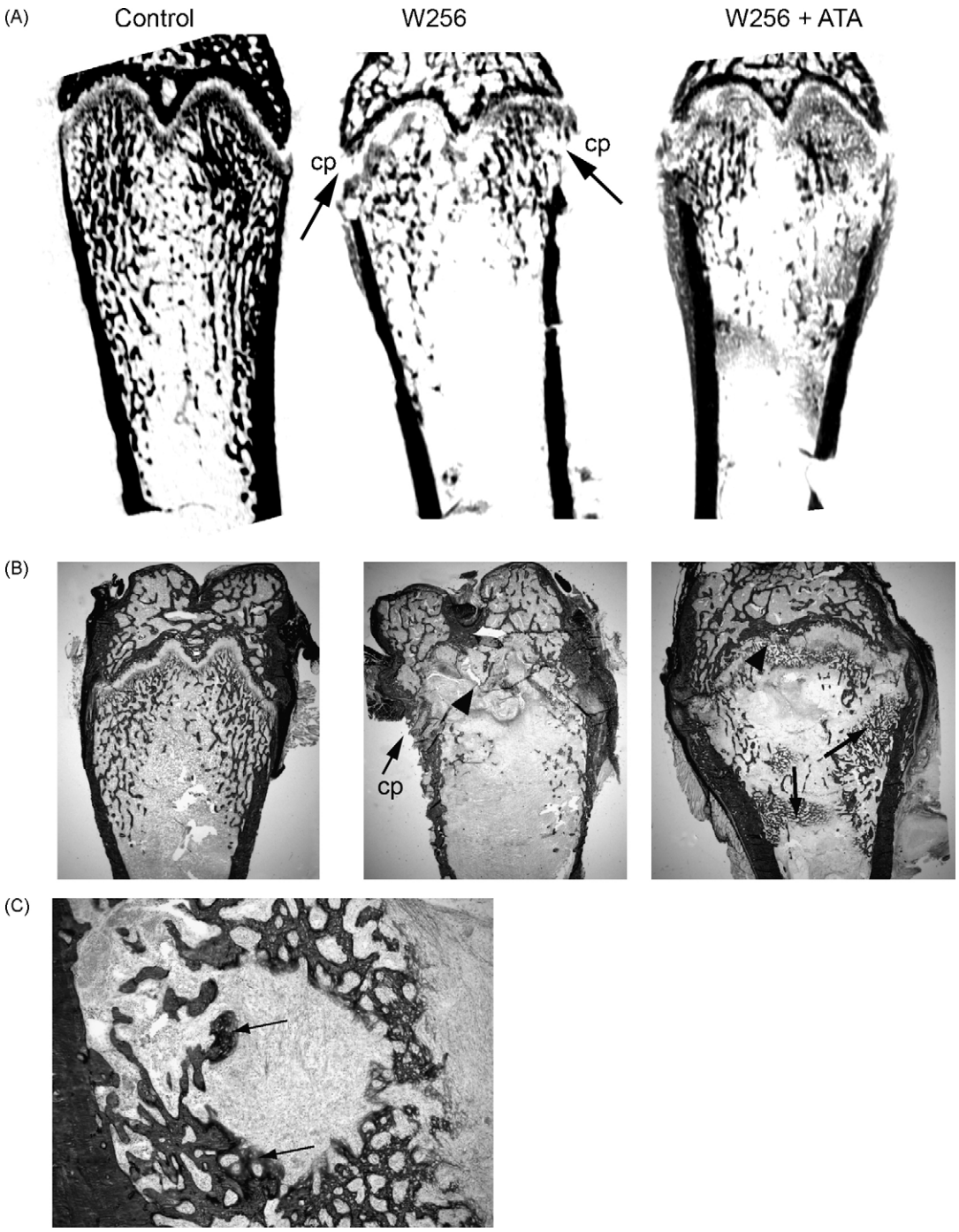

Fig. 1. (A) 2D MicroCT imaging of the right femurs 20 days after surgery in the control, W256 and W256 + ATA groups. 3D models were re-sliced across a plane positioned vertical and parallel to the long axis of the femur. Note the large and irregular band of bone loss below the growth plate in W256 animals. Cortical perforations (cp) are evidenced in the W256 group near the groove of Ranvier. (B) Histological analysis of corresponding bones. Arrows evidenced multiple foci of newly apposed bone (metaplasia) at the surface of trabeculae and endosteum in the W256 + ATA group. Arrowheads illustrate the resorption of cartilage in the growth plate of W256 and W256 + ATA groups; a cortical perforation is evidenced (cp). Goldner's trichrome, original magnification: 12.5×. (C) Histological analysis of an area of newly apposed bone in the W256 + ATA group. Arrows illustrate the osteoid tissue. Goldner's trichrome, original magnification: 100×.

Walker 256/B cells is a very reproducible method to induce skeletal metastases [3,5]. W256 cells can be maintained and propagated *in vitro* or *in vivo* by repetitive subcutaneous [32], intramuscular [33] or ascitic passages [34]. After injection, cultured W256 cells are only susceptible to develop subcutaneously, intramuscularly or in ascite but cannot induce bone metastases. Two passages *in vivo* are required before cells can induce bone metastases in the recipient animals [3]. Cytokine content is known to be considerably modified in ascitic fluids in presence of cancer cells [35]. In this study, Walker 256/B cells caused osteolytic metastases associated with marked alterations of bone microarchitecture as previously described [4].

To our knowledge, there is no report about to what extent metastatic cancer cells disturb the oxidative/antioxidative system in the bone microenvironment. In the recent years, there has been a growing interest in studying the role played by oxidative stress in cancer initiation and progression [11,12,36]. Cancer initiation and progression are reported to lower antioxidant defences in bone cells and cause bone loss [37,38]. Increased oxidative stress and

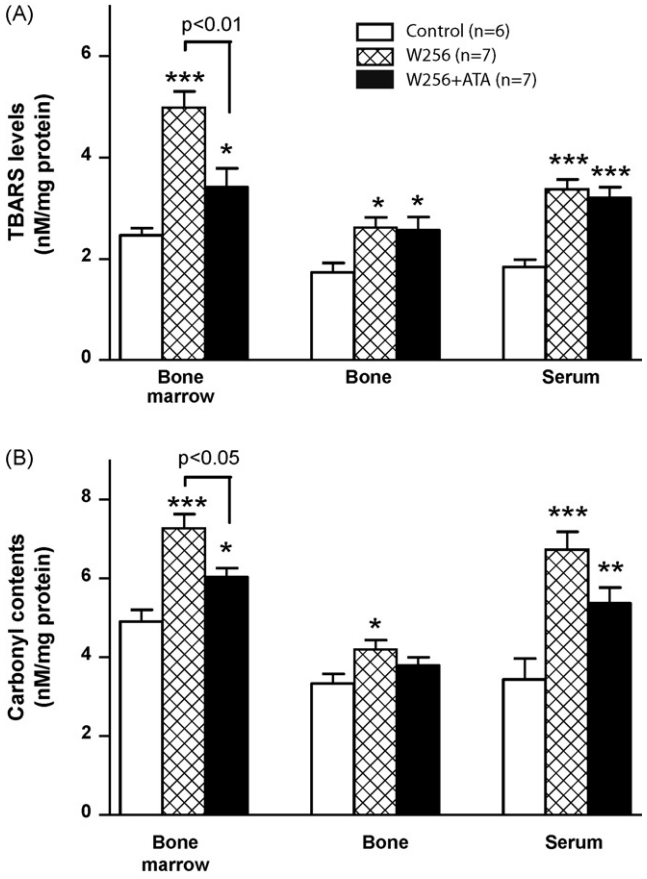

Fig. 2. (A) Lipid peroxidation level in bone marrow, bone, and serum in the control ($n = 6$), W256 ($n = 7$), and W256 + ATA ($n = 7$) groups. Lipid peroxidation was determined using TBARS assay. Statistical significance of the differences: control versus W256 $^{*}p < 0.05$, $^{**}p < 0.01$, $^{***}p < 0.001$. (B) Carbonyl contents in bone marrow, bone, and serum in the control ($n = 6$), W256 ($n = 7$), and W256 + ATA ($n = 7$) groups. Protein oxidation was determined using a spectrometric DNPH assay. Statistical significance of the differences: control versus W256 $^{*}p < 0.05$, $^{**}p < 0.01$, $^{***}p < 0.001$.

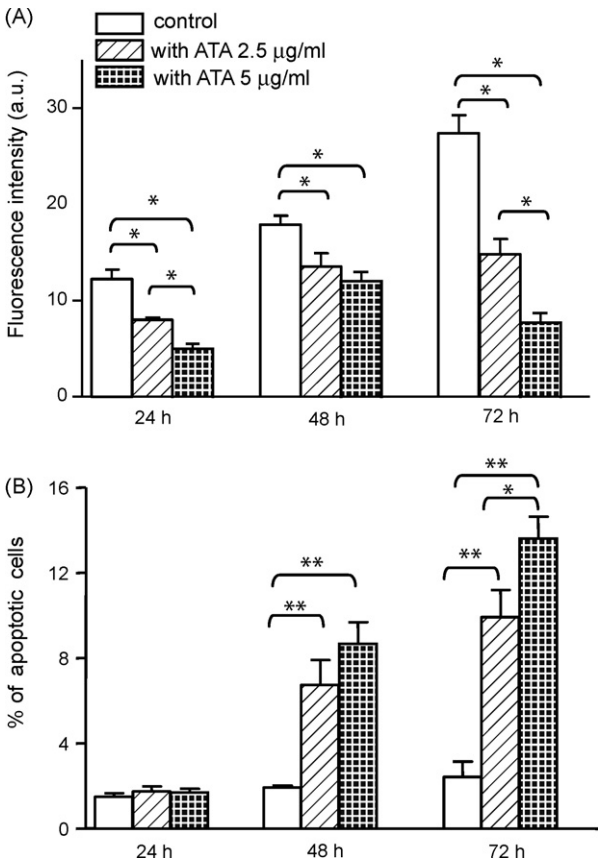

Fig. 3. (A) Time course and dose–response effects of ATA on fluorescence signal intensity of 2′,7′-dichlorofluorescein (DCF) formed by Walker 256/B cells in culture. Statistical significance of differences: $^{*}p < 0.05$. (B) Time course and dose–response effects of ATA on Walker 256/B cell apoptosis in culture. Statistical significance of differences: $^{*}p < 0.05$. $^{**}p < 0.01$.

lipid peroxidation have been reported in benign and malignant breast tissues [12]. Lipid peroxidation is believed to be an important cause of destruction and damage to cell membranes and to alter physiological and biochemical characteristics of biological systems by the development of oxygen radicals-mediated time damage [39–42]. The action of cytotoxic end-products of lipid and protein oxidation may potentate tissues injury [43].

It is known that high levels of oxidant production perturb the normal redox balance and shift cells into a state of oxidative stress by depletion of antioxidant systems [44]. Depletions in SOD and GSH-p confirm that these enzymes are used as antioxidants against free-radical production. In human, the total antioxidant capacity is decreased in cancerous patients [45].

It is likely that there is a strong relationship between oxidative stress and bone loss. Garrett et al. reported that oxidative stress is involved in osteoclastogenesis and bone resorption [46,47]. An oxidative stress has been shown to inhibit osteoblastic differentiation via ERK (extracellular signal-regulated kinases) and ERK-dependant NF-κB signaling pathway [48,49]. Activation of nuclear factor-κB (NF-κB) plays an important role in osteoclastogenesis [47,50]. A negative correlation has been found between oxidative stress and bone mineral density in aged men and women [51]. In normal healthy conditions, active osteoclasts generate large quantities of ROS during bone physiological resorption [52].

In our study, rats with bone metastases exhibited an increased oxidative stress and lipid peroxidation. The important lipoperoxidation outlined in the bone marrow could be due to the tumor cells. Levels of peroxidated lipids and protein in bone, bone marrow and serum were considerably increased in the W256 group; this could be an additional cause that increased osteoclastogenesis in the bone marrow microenvironment [53]. This could be due to the higher cell and lipid content in the bone marrow than in bone itself. Lipid peroxidation and protein oxidation were accompanied by a significant reduction in the enzymatic antioxidant levels (SOD and GSH-p) in bone and bone marrow. Walker 256/B cells unbalanced of the oxidative/antioxidative status, via exaggeration of ROS production. When we examined the status of DCF in Walker 256/B cells in culture following ATA treatment, we observed a considerable decrease in the intensity of fluorescence. This concurs with previous study in rats by Yun et al. [15] both *in vivo* and *in vitro* administration of vitamin E (DL-α-tocopherol) showed protective effect against damage caused by PCB via ROS expression. A previous study by Yu et al. [54] indicated that *in vitro* exposure to different forms of vitamin E during 3 days induced MCF-7 and MDA-MB-435 human breast cancer cells to undergo apoptosis. In the present study, ATA at the doses of 2.5 and 5 μl/ml induced a significant increase in the number of apoptotic cells that parallels the decrease of ROS measured biochemically [55].

Antioxidants are molecules that prevent or reduce the extent of oxidative destruction of biomolecules [7]. It has been shown that dietary antioxidant vitamin intake has beneficial effects on bone marrow in postmenopausal women [56]. A marked decrease in plasma antioxidants was found in patients with severe bone loss [57]. In a recent study, supplementation with vitamin E prevented or reduced the irradiation-induced oxidative stress in skeletal muscles and bones [58]. Vitamin E is a soluble antioxidant that is

incorporated into cell membranes to prevent lipid peroxidation [59]. It has multiple potential anti-carcinogenic effects including its antioxidant properties with free-radical scavenging and lipid peroxidation prevention [60,61]. Vitamin E also prevents activation of monocytes or other cytokine-secreting cells present at a relative high level in bone marrow [62].

In our study, ATA reduced the oxidative injury in the bone microenvironment, as assessed by several oxidative stress dosages. Owing to its antioxidant activity, ATA restored some antioxidant levels significantly, especially bone GSH-p, an antioxidant enzyme predominantly expressed by osteoclasts [38]. However, since TBARS and CC levels remained at higher levels in W256 + ATA rats it is likely that the dose used in this study did not had a full protective effect. The effect of vitamin E appeared to modify the tumor mass in the bone with areas of tumor necrosis and foci of osteosclerotic woven bone forming irregular networks anchored on pre-existing trabeculae or the endosteum.

In conclusion, mammary gland carcinoma cells have adverse effects on bone microenvironment. Walker 256/B cells induced bone loss, increased the oxidative stress and impaired the bone microenvironment antioxidant system. The effects are complex, and appear to demonstrate regional differences. ATA proved to be partially beneficial in reducing the oxidative stress damage and the bone loss. Vitamin E induced osteosclerosis in this rat model by enhancing metaplastic bone apposition. Further studies will evaluate the combined effect ATA and other bone sparing agents such as bisphosphonates.

Conflict of interest

None declared.

Acknowledgments

The authors are greatly indebted to G. Brossard and N. Gaborit for their help with X-ray microCT and F. Pascaretti for the histological technique. This work was supported by the 99/UR/0860 Tunisia, INSERM and Contrat de recherche Région Pays de la Loire (France), Bioregos.

References

[1] G.R. Mundy, Metastasis to bone: causes, consequences and therapeutic opportunities, Nat. Rev. Cancer 2 (8) (2002) 584–593.
[2] R.E. Coleman, Metastatic bone disease: clinical features, pathophysiology and treatment strategies, Cancer Treat. Rev. 27 (3) (2001) 165–176.
[3] S. Blouin, M.F. Baslé, D. Chappard, Rat models of bone metastases, Clin. Exp. Metastasis 22 (8) (2005) 605–614.
[4] S. Blouin, M.F. Moreau, M.F. Baslé, D. Chappard, Relations between radiograph texture analysis and microcomputed tomography in two rat models of bone metastases, Cells Tissues Organs 182 (3–4) (2006) 182–192.
[5] Q.L. Mao-Ying, J. Zhao, Z.Q. Dong, J. Wang, J. Yu, M.F. Yan, Y.Q. Zhang, G.C. Wu, Y.Q. Wang, A rat model of bone cancer pain induced by intra-tibia inoculation of Walker 256 mammary gland carcinoma cells, Biochem. Biophys. Res. Commun. 345 (4) (2006) 1292–1298.
[6] T. Hahn, L. Szabo, M. Gold, L. Ramanathapuram, L.H. Hurley, E.T. Akporiaye, Dietary administration of the proapoptotic vitamin E analogue {alpha}-tocopheryloxyacetic acid inhibits metastatic murine breast cancer, Cancer Res. 66 (19) (2006) 9374–9378.
[7] P.M. Abuja, R. Albertini, Methods for monitoring oxidative stress, lipid peroxidation and oxidation resistance of lipoproteins, Clin. Chim. Acta 306 (1–2) (2001) 1–17.
[8] E. Niki, Y. Yoshida, Y. Saito, N. Noguchi, Lipid peroxidation: mechanisms, inhibition, and biological effects, Biochem. Biophys. Res. Commun. 338 (1) (2005) 668–676.
[9] P.A. Cerutti, B.F. Trump, Inflammation and oxidative stress in carcinogenesis, Cancer Cells 3 (1) (1991) 1–7.
[10] R. Badraoui, Z. Sahnoun, N.B. Bouayed, A. Hakim, T. Rebai, May antioxidant status depletion by tetradifon induce secondary genotoxicity in female wistar rat via oxidative stress? Pesticide Biochem. Physiol. 88 (2007) 149–155.
[11] S.S. Khanzode, M.G. Muddeshwar, S.D. Khanzode, G.N. Dakhale, Antioxidant enzymes and lipid peroxidation in different stages of breast cancer, Free Radic. Res. 38 (1) (2004) 81–85.
[12] A. Gonenc, D. Erten, S. Aslan, M. Akinci, B. Simsek, M. Torun, Lipid peroxidation and antioxidant status in blood and tissue of malignant breast tumor and benign breast disease, Cell Biol. Int. 30 (4) (2006) 376–380.
[13] Y. Henrotin, B. Kurz, Antioxidant to treat osteoarthritis: dream or reality? Curr. Drug Targets 8 (2) (2007) 347–357.
[14] Y.L. Tain, G. Freshour, A. Dikalova, K.K. Griendling, C. Baylis, Vitamin, E reduces glomerulosclerosis, restores renal neuronal NOS, and suppresses oxidative stress in the 5/6 nephrectomized rat, Am. J. Physiol. Renal Physiol. 292 (2007) 1404–1410.
[15] J.S. Yun, H.K. Na, K.S. Park, Y.H. Lee, E.Y. Kim, S.Y. Lee, J.I. Kim, J.H. Kang, D.S. Kim, K.H. Choi, Protective effects of vitamin E on endocrine disruptors, PCB-induced dopaminergic neurotoxicity, Toxicology 216 (2–3) (2005) 140–146.
[16] H.J. Kim, E.J. Chang, H.M. Kim, S.B. Lee, H.D. Kim, G. Su Kim, H.H. Kim, Antioxidant alpha-lipoic acid inhibits osteoclast differentiation by reducing nuclear factor-kappaB DNA binding and prevents in vivo bone resorption induced by receptor activator of nuclear factor-kappaB ligand and tumor necrosis factor-alpha, Free Radic. Biol. Med. 40 (9) (2006) 1483–1493.
[17] J.A. Drisko, J. Chapman, V.J. Hunter, The use of antioxidants with first-line chemotherapy in two cases of ovarian cancer, J. Am. Coll. Nutr. 22 (2) (2003) 118–123.
[18] J.A. Drisko, J. Chapman, V.J. Hunter, The use of antioxidant therapies during chemotherapy, Gynecol. Oncol. 88 (3) (2003) 434–439.
[19] J. Serra, P. Soille, Mathematical morphology and its applications to image processing, Kluwer Academic Publisher, Dordrecht, 1994.
[20] M. Hahn, M. Vogel, M. Pompesius-Kempa, G. Delling, Trabecular bone pattern factor—a new parameter for simple quantification of bone microarchitecture, Bone 13 (4) (1992) 327–330.
[21] D. Chappard, Technical aspects: How do we best prepare bone samples for proper histological analysis? in: D. Heymann (Ed.), Bone cancer: progression and therapeutic approaches, Academic Press, London, UK, 2009, pp. 203–210.
[22] T.P. Devasagayam, U. Tarachand, Decreased lipid peroxidation in the rat kidney during gestation Biochem. Biophys. Res. Commun. 145 (1) (1987) 134–138.
[23] T.F. Slater, B.C. Sawyer, The stimulatory effects of carbon tetrachloride and other halogenoalkanes on peroxidative reactions in rat liver fractions in vitro. General features of the systems used, Biochem. J. 123 (5) (1971) 805–814.
[24] J.M. Fagan, B.G. Sleczka, I. Sohar, Quantitation of oxidative damage to tissue proteins, Int. J. Biochem. Cell Biol. 31 (7) (1999) 751–757.
[25] R.F. Beers Jr., I.W. Sizer, A spectrophotometric method for measuring the breakdown of hydrogen peroxide by catalase, J. Biol. Chem. 195 (1) (1952) 133–140.
[26] E. Beutler, F. Matsumoto, Ethnic variation in red cell glutathione peroxidase activity, Blood 46 (1) (1975) 103–110.
[27] J.M. McCord, I. Fridovich, The utility of superoxide dismutase in studying free radical reactions. I. Radicals generated by the interaction of sulfite, dimethyl sulfoxide, and oxygen, J. Biol. Chem. 244 (22) (1969) 6056–6063.
[28] K. Gunawardena, D.K. Murray, A.W. Meikle, Vitamin E and other antioxidants inhibit human prostate cancer cells through apoptosis, Prostate 44 (4) (2000) 287–295.
[29] J.A. Royall, H. Ischiropoulos, Evaluation of 2′,7′-dichlorofluorescin and dihydrorhodamine 123 as fluorescent probes for intracellular H2O2 in cultured endothelial cells, Arch. Biochem. Biophys. 302 (2) (1993) 348–355.
[30] H. Wang, J.A. Joseph, Quantifying cellular oxidative stress by dichlorofluorescein assay using microplate reader, Free Radic. Biol. Med. 27 (5–6) (1999) 612–616.
[31] T.A. Guise, G.R. Mundy, Cancer and bone, Endocr. Rev. 19 (1998) 18–54.
[32] D. Stepensky, G. Golomb, A. Hoffman, Pharmacokinetic and pharmacodynamic evaluation of intermittent versus continuous alendronate administration in rats, J. Pharm. Sci. 91 (2) (2002) 508–516.
[33] R. Rizzoli, H. Fleisch, The Walker 256/B carcinosarcoma in thyroparathyroidectomized rats: a model to evaluate inhibitors of bone resorption, Calcif. Tissue Int. 41 (4) (1987) 202–207.
[34] B. Krempien, C. Manegold, Prophylactic treatment of skeletal metastases, tumor-induced osteolysis, and hypercalcemia in rats with the bisphosphonate Cl_2MBP, Cancer 72 (1) (1993) 91–98.
[35] A. Takagane, M. Terashima, K. Abe, M. Araya, S. Nishizuka, K. Saito, Induction of cytokines in ascitic fluid by intraperitoneal OK-432 administration in patients with gastric cancer, J. Jpn. Soc. Cancer Ther. 31 (11) (1996) 1067–1074.
[36] A. Gonenc, Y. Ozkan, M. Torun, B. Simsek, Plasma malondialdehyde (MDA) levels in breast and lung cancer patients, J. Clin. Pharm. Ther. 26 (2) (2001) 141–144.
[37] J.M. Lean, J.T. Davies, K. Fuller, C.J. Jagger, B. Kirstein, G.A. Partington, Z.L. Urry, T.J. Chambers, A crucial role for thiol antioxidants in estrogen-deficiency bone loss, J. Clin. Invest. 112 (6) (2003) 915–923.
[38] C.J. Jagger, J.M. Lean, J.T. Davies, T.J. Chambers, Tumor necrosis factor-alpha mediates osteopenia caused by depletion of antioxidants, Endocrinology 146 (1) (2005) 113–118.
[39] H. Kaya, N. Delibas, M. Serteser, E. Ulukaya, O. Ozkaya, The effect of melatonin on lipid peroxidation during radiotherapy in female rats, Strahlenther Onkol 175 (6) (1999) 285–288.
[40] M.F. Moreau, Y. Gallois, M.F. Baslé, D. Chappard, Gamma irradiation of human bone allografts alters medullary lipids and releases toxic compounds for osteoblast-like cells, Biomaterials 21 (4) (2000) 369–376.
[41] A.M. Gamal el-din, A.M. Mostafa, O.A. Al-Shabanah, A.M. Al-Bekairi, M.N. Nagi, Protective effect of arabic gum against acetaminophen-induced hepatotoxicity in mice, Pharmacol. Res. 48 (6) (2003) 631–635.

[42] G. Sener, A.O. Sehirli, G. Ayanoglu-Dulger, Protective effects of melatonin, vitamin E and N-acetylcysteine against acetaminophen toxicity in mice: a comparative study, J. Pineal Res. 35 (1) (2003) 61–68.
[43] G. Sener, O. Sehirli, S. Cetinel, B.G. Yegen, N. Gedik, G. Ayanoglu-Dulger, Protective effects of MESNA (2-mercaptoethane sulphonate) against acetaminophen-induced hepatorenal oxidative damage in mice, J. Appl. Toxicol. 25 (1) (2005) 20–29.
[44] T. Finkel, N.J. Holbrook, Oxidants, oxidative stress and biology of ageing, Nature 408 (2000) 147–239.
[45] X. Liu, J. Zhao, R. Zheng, DNA damage of tumor-associated lymphocytes and total antioxidant capacity in cancerous patients, Mutat. Res. 539 (1–2) (2003) 1–8.
[46] I.R. Garrett, B.F. Boyce, R.O. Oreffo, L. Bonewald, J. Poser, G.R. Mundy, Oxygen-derived free radicals stimulate osteoclastic bone resorption in rodent bone in vitro and in vivo, J. Clin. Invest. 85 (3) (1990) 632–639.
[47] J.H. Fraser, M.H. Helfrich, H.M. Wallace, S.H. Ralston, Hydrogen peroxide, but not superoxide, stimulates bone resorption in mouse calvariae, Bone 19 (3) (1996) 223–226.
[48] N. Mody, F. Parhami, T.A. Sarafian, L.L. Demer, Oxidative stress modulates osteoblastic differentiation of vascular and bone cells, Free Radic. Biol. Med. 31 (4) (2001) 509–519.
[49] X.C. Bai, D. Lu, J. Bai, H. Zheng, Z.Y. Ke, X.M. Li, S.Q. Luo, Oxidative stress inhibits osteoblastic differentiation of bone cells by ERK and NF-kappaB, Biochem. Biophys. Res. Commun. 314 (1) (2004) 197–207.
[50] V. Iotsova, J. Caamano, J. Loy, Y. Yang, A. Lewin, R. Bravo, Osteopetrosis in mice lacking NF-kappaB1 and NF-kappaB2, Nat. Med. 3 (11) (1997) 1285–1289.
[51] S. Basu, K. Michaelsson, H. Olofsson, S. Johansson, H. Melhus, Association between oxidative stress and bone mineral density, Biochem. Biophys. Res. Commun. 288 (1) (2001) 275–279.
[52] M.J. Steinbeck, W.H. Appel Jr., A.J. Verhoeven, M.J. Karnovsky, NADPH-oxidase expression and in situ production of superoxide by osteoclasts actively resorbing bone, J. Cell Biol. 126 (3) (1994) 765–772.
[53] T.A. Guise, Molecular mechanisms of osteolytic bone metastases, Cancer 88 (12S) (2000) 2892–2898.
[54] W. Yu, M. Simmons-Menchaca, A. Gapor, B.G. Sanders, K. Kline, Induction of apoptosis in human breast cancer cells by tocopherols and tocotrienols, Nutr. Cancer 33 (1) (1999) 26–32.
[55] K.A. Lawson, K. Anderson, R.M. Snyder, M. Simmons-Menchaca, J. Atkinson, L.Z. Sun, A. Bandyopadhyay, V. Knight, B.E. Gilbert, B.G. Sanders, K. Kline, Novel vitamin E analogue and 9-nitro-camptothecin administered as liposome aerosols decrease syngeneic mouse mammary tumor burden and inhibit metastasis, Cancer Chemother. Pharmacol. 54 (5) (2004) 421–431.
[56] D.J. Morton, E.L. Barrett-Connor, D.L. Schneider, Vitamin, C supplement use and bone mineral density in postmenopausal women, J. Bone Miner. Res. 16 (1) (2001) 135–140.
[57] D. Maggio, M. Barabani, M. Pierandrei, M.C. Polidori, M. Catani, P. Mecocci, U. Senin, R. Pacifici, A. Cherubini, Marked decrease in plasma antioxidants in aged osteoporotic women: results of a cross-sectional study, J. Clin. Endocrinol. Metab. 88 (4) (2003) 1523–1527.
[58] S. Yilmaz, E. Yilmaz, Effects of melatonin and vitamin E on oxidative-antioxidative status in rats exposed to irradiation, Toxicology 222 (1–2) (2006) 1–7.
[59] E. Niki, N. Noguchi, Dynamics of antioxidant action of vitamin E, Acc. Chem. Res. 37 (1) (2004) 45–51.
[60] R. Brigelius-Flohe, M.G. Traber, Vitamin E: function and metabolism, Faseb J. 13 (10) (1999) 1145–1155.
[61] K.S. Choi, M.K. Bae, J.W. Jeong, H.E. Moon, K.W. Kim, Hypoxia-induced angiogenesis during carcinogenesis, J. Biochem. Mol. Biol. 36 (1) (2003) 120–127.
[62] N.S. Ahmad, B.A. Khalid, D.A. Luke, S. Ima Nirwana, Tocotrienol offers better protection than tocopherol from free radical-induced damage of rat bone, Clin. Exp. Pharmacol. Physiol. 32 (9) (2005) 761–770.